Initiation of cofilin activity in response to EGF is uncoupled from cofilin phosphorylation and dephosphorylation in carcinoma cells

Xiaoyan Song, Xiaoming Chen, Hideki Yamaguchi, Ghassan Mouneimne, John S. Condeelis and Robert J. Eddy*

Department of Anatomy and Structural Biology, Albert Einstein College of Medicine of Yeshiva University, F628, 1300 Morris Park Avenue, Bronx, New York, NY 10461, USA

*Author for correspondence (e-mail: roeddy@aecom.yu.edu)

Accepted 13 April 2006
Journal of Cell Science 119, 2871-2881 Published by The Company of Biologists 2006
doi:10.1242/jcs.03017

Summary

It has been demonstrated that the actin-severing activity of cofilin can be downregulated by LIM kinase (LIMK)-dependent phosphorylation at residue Ser3. Chemotactic stimulaton in various cell types induces cofilin dephosphorylation, suggesting that cofilin activation in these cells occurs by a dephosphorylation mechanism. However, resting metastatic carcinoma cells have the majority of their cofilin in a dephosphorylated but largely inactive state. Stimulation with epidermal growth factor (EGF) induces an increase in cofilin activity after 60 seconds together with an increase in phosphorylated cofilin (p-cofilin), indicating that cofilin dephosphorylation is not coupled to cofilin activation in these cells. Suppression of LIMK function by inhibiting Rho-associated protein kinase (ROCK) or LIMK siRNA inhibited the EGF-induced cofilin phosphorylation but had no effect on cofilin activity or cofilin-dependent lamellipod protrusion induced by EGF. Correlation analysis revealed that cofilin, p-cofilin and LIMK are not colocalized, and changes in the location of these proteins upon stimulation with EGF indicate that they are not functionally coupled. Phospholipase C, which has been implicated in cofilin activation following stimulation with EGF, does not regulate p-cofilin levels following stimulation with EGF. Therefore, our results do not support a model for the initial activation of cofilin by dephosphorylation in response to chemoattractant stimulation in metastatic carcinoma cells.

Key words: LIM kinase, Cofilin-severing, Rho-associated protein kinase

Introduction

In a variety of crawling cells, the cofilin/ADF proteins have been implicated in the dynamics of the actin cytoskeleton at the plasma membrane during cell protrusions (Bamburg, 1999; Condeelis, 2001; Mouneimne et al., 2004; Ono et al., 1993; Pollard and Borisy, 2003) and chemotaxis (Mouneimne et al., 2004). Owing to its ability to sever actin filaments, cofilin can play a central role in the generation of actin nucleation sites directly, by the generating free barbed-filament ends (Chan et al., 2000; Du and Frieden, 1998; Ichetovkin et al., 2000; Maciver et al., 1998). This hypothesis has been tested directly in carcinoma cells by using a caged analog of cofilin that cannot be phosphorylated (Ghosh et al., 2002). Photoactivation of caged cofilin produced increases in barbed ends and F-actin in vivo, and produces protrusions at the site of uncaging, demonstrating that the severing activity of cofilin is sufficient to drive actin polymerization and protrusion, and to set the direction of cell migration (Ghosh et al., 2004). These results place cofilin in a central position in regulating cell direction during chemotaxis.

The essential role of cofilin in the initiation of actin polymerization and protrusion suggests that a chemotactic cell must possess a high degree of temporal and spatial regulation over the severing activity of cofilin. Cofilin can be inactivated by phosphorylation of Ser3 by the LIM or TES family of kinases. LIM kinase 1 and 2 (LIMK1 and LIMK 2) are regulated by Rho GTPases through their downstream effectors Rho-associated protein kinase (ROCK) and p21-activated kinases 1 and 4 (PAK1 and PAK4), which activate LIMK1 and LIMK2 by phosphorylation at residues Thr508 and Thr505, respectively (Edwards et al., 1999; Maekawa et al., 1999; Ohashi et al., 2000). In invasive carcinoma cells, LIMK1 is upregulated and is the most abundant and dominant cofilin kinase (Wang et al., 2004).

The protein phosphatase Slingshot (SSH) and the new haloacid dehalogenase (HAD)-family phosphatase chronophin (CIN), have been proposed to be the primary activators of cofilin by dephosphorylation at Ser3 in a variety of cell types (Gohla et al., 2005; Niwa et al., 2002). Cofilin is also inactivated by binding to phosphatidylinositol (4,5)-bisphosphate [PtdIns(4,5)P_2] in vitro (Ojala et al., 2001; Yonezawa et al., 1991; Yonezawa et al., 1990). However, the role of phosphoinositides in cofilin activation during chemoattractant-elicited cell protrusion in vivo is largely unexplored.

If the dephosphorylation of cofilin is – as proposed – the primary mechanism for the initiation of cofilin activity in vivo (Bamburg, 1999; Nishita et al., 2005), cofilin dephosphorylation would be expected to precede all cofilin-dependent motility events following stimulation. However, the phosphorylation status of cofilin before and after stimulation

seems to vary in different cell types. In neuronal cells and neutrophils, the majority of cofilin is held in an inactive, phosphorylated pool prior to stimulation (Meberg et al., 1998; Moriyama et al., 1996). Stimulation with a variety of growth factors and chemotactic agents induces dephosphorylation of cofilin (Kanamori et al., 1995; Meberg et al., 1998; Okada et al., 1996). However, in T-lymphocytes and Jurkat cells, stimulation with stromal cell-derived factor 1α (SDF-1α) causes cofilin phosphorylation (Nishita et al., 2002), whereas in A431 and 3T3 cells stimulation with epidermal growth factor (EGF) causes increases in both the rates of dephosphorylation and phosphorylation, which cancel each other (Meberg et al., 1998). Moreover, the activity status of cofilin in these stimulated cells has not been assessed. Such wide differences in the patterns of cofilin dephosphorylation between cell types during stimulation and also the absence of data on cofilin activity make it difficult to ascertain the significance of changes in the cofilin phosphorylation status in cells during the stimulation of actin polymerization in vivo. Therefore, the pattern of cofilin phosphorylation and/or dephosphorylation needs to be described and related to cofilin activity directly, following stimulation in a single cell type to determine whether dephosphorylation is responsible for activating cofilin. A complete understanding at this level is important for breast tumor cells because cofilin activation has a dominant effect in determining cell direction in tumor cells (Ghosh et al., 2004; Mouneimne et al., 2004). In addition, the invasion signature of breast carcinoma cells predicates that cofilin activity is an important contributor to the metastatic phenotype (Wang et al., 2004); this has been demonstrated directly in animal models where cofilin activity determines metastatic outcome in mammary tumors (Wang et al., 2006). These results emphasize that the regulation of cofilin needs to be understood to predict metastatic outcome.

Therefore, to explore the importance of the phosphorylation status of cofilin during the activation of cofilin in metastatic tumor cells, we undertook a study of the changes in cofilin phosphorylation status upon stimulation with EGF. Our data do not support a model for the initial activation of cofilin-severing by dephosphorylation and suggest additional mechanisms of regulation.

Results

Cofilin-dependent severing activity increases after stimulation with EGF

Previous studies have described the generation of two distinct actin polymerization transients following stimulation with EGF (Chan et al., 2000; Chan et al., 1998; Mouneimne et al., 2004). These transients are closely associated with the generation of two peaks of free barbed ends as measured in an in situ barbed-end assay. The first or early peak of barbed ends occurs at 60 seconds post-EGF, whereas a later peak occurs at three minutes post-EGF. To address the relative contribution of cofilin severing activity to the generation of free barbed ends, we employed an in vitro fluorescent F-actin-severing assay as described in Materials and Methods, and quantified the relative severing activity in cell lysates prepared at various times after stimulation with EGF. In unstimulated cells, a low level of severing activity was detected. After stimulation with EGF, a peak of actin-severing activity was detected at 60 seconds after EGF addition, corresponding with the early peak of barbed-end activity. This peak of actin-severing activity averaged 3.2-fold above unstimulated levels and decayed toward baseline levels by approximately 3 minutes. To determine whether the peak of severing activity at 60 seconds was cofilin-specific, we performed a severing assay in the presence of a cofilin function-blocking antibody. This antibody was originally raised against the actin-binding site of cofilin and has been shown to effectively block the in vitro severing activity of purified cofilin (Chan et al., 2000). The relative amount of actin-severing activity at 60 seconds post-stimulation with EGF was significantly reduced to unstimulated levels in the presence of the function-blocking antibody, whereas a non-specific IgG had no inhibitory effect (Fig. 1B). Furthermore, the phosphatase inhibitor Na_3VO_4 alone or together with NaF was added to the cell lysis buffer to determine whether dephosphorylation, which might occur in the cell lysate, contributes to cofilin activation. As shown in Fig. 1C,D, neither the activity nor phosphorylation of cofilin was altered in the cell lysate in the presence of these phosphatase inhibitors. The proposed cofilin phosphatase SSH is sensitive to Na_3VO_4 (Niwa et al., 2002), whereas CIN has been shown to be sensitive to both NaF and Na_3VO_4 (Gohla et al., 2005). These data indicate that the peak of severing activity detected at 60 seconds is caused by cofilin and that the activation of cofilin does not occur in the cell lysate due to unchecked dephosphorylation.

Cofilin activation is not temporally correlated with cofilin dephosphorylation after stimulation with EGF

The peak of cofilin activity at 60 seconds after EGF stimulation seen in Fig. 1 has been shown to be required for the early barbed-end transient that occurs at 60 seconds and is involved in directional sensing of EGF during chemotaxis (Mouneimne et al., 2004). Therefore, it was important to determine whether this peak of cofilin activity is correlated with cofilin dephosphorylation, as predicted by the dephosphorylation model of cofilin activation (Okada et al., 1996; Zhan et al., 2003). To investigate whether metastatic carcinoma cells regulate cofilin by a similar dephosphorylation mechanism in response to growth factor stimulation, we monitored the change in cofilin phosphorylation following EGF stimulation, by three independent methods: western blotting of cell lysates separated by SDS-PAGE, isoelectric focusing gel (IEF) and immunofluorescence with a phosphorylated cofilin (p-cofilin)-specific antibody. MTLn3 cell lysates prepared at various times after EGF stimulation and western blotted with p-cofilin-specific antibodies showed an average 2.2-fold increase in the p-cofilin content by 60 seconds. After peaking at 60 seconds, p-cofilin levels remained elevated for 5 minutes following stimulation with EGF, and gradually returned to pre-stimulation levels by 30 minutes (Fig. 2B,C). To confirm this result, we assessed the changes in the ratio of dephosphorylated cofilin to p-cofilin following EGF stimulation. Isoelectric focusing gel analysis of MTLn3 lysates revealed that p-cofilin accounts for only 18±4% of the total cofilin in resting cells in cultures, at densities (<50% confluence) used for stimulation with chemoattractants. The amount of p-cofilin increases approximately twofold at 60 seconds (to 37±6%) following stimulation with EGF (Fig. 2A). In support of these observations, the total intensity of cellular p-cofilin staining, measured in fixed cells

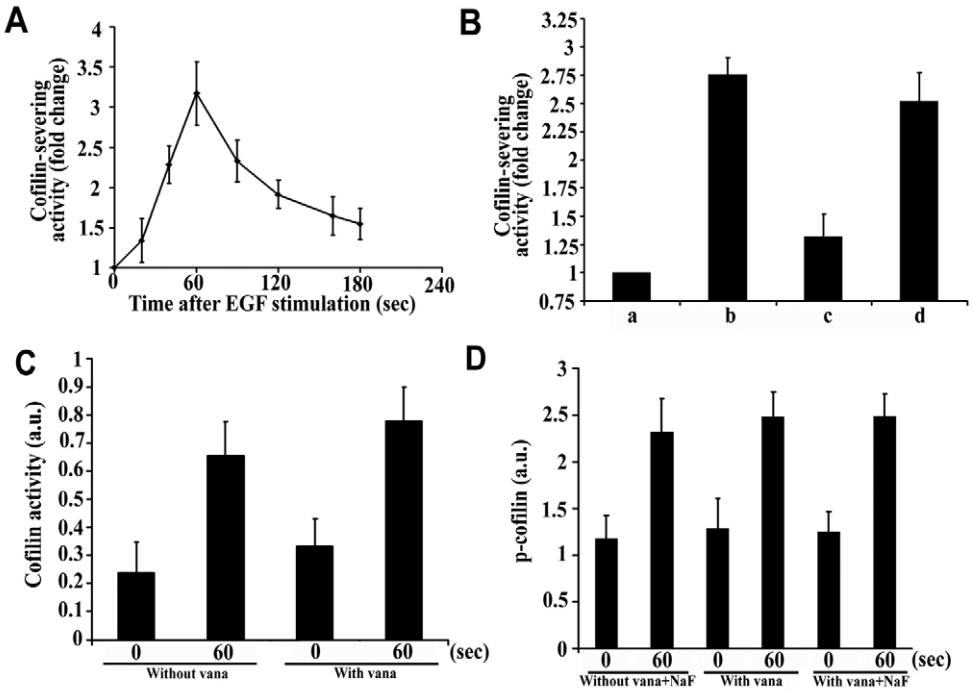

Fig. 1. Cofilin severing is activated in the leading edge and its severing activity peaks at 60 seconds after stimulation with EGF. (A) Severing activity in cell lysates prepared at the times shown after addition of EGF was measured in an F-actin-severing assay. (Error bars indicate the standard error of the mean (s.e.m.) (B) Pre-incubation of cell lysates with an antibody that blocks cofilin-severing activity abolished the severing-activity peak at 60 seconds after stimulation with EGF (c). However, pre-incubation of nonspecific IgG (d) had no effect on the severing activity peak at 60 seconds after stimulation with EGF, demonstrating that cofilin is the severing protein activated in the cell lysates. Severing activity in the same experiment at 0 seconds (a) and 60 seconds (b) after stimulation with EGF is shown for comparison. (Error bars indicate the s.e.m.) (C) Cofilin-severing acitivity in cell lysates prepared with or without Na_3VO_4 at the times shown after addition of EGF was measured in an F-actin-severing assay. (D) Changes in the amounts of phosphorylated cofilin with or without the addition of Na_3VO_4 and NaF.

by immunofluorescence with a p-cofilin-specific antibody, increased approximately twofold at 60 seconds (Fig. 3B).

Increase in dephosphorylated cofilin after EGF stimulation is not spatially coupled to decrease in p-cofilin

To obtain spatial information where changes in dephosphorylated cofilin and p-cofilin occur in the cell, a detailed analysis of the immunolocalization patterns in MTLn3 cells at 0 and 60 seconds after EGF stimulation was undertaken. The localization of dephosphorylated cofilin was visualized by subtracting the scaled staining pattern of p-cofilin from the pattern of total cofilin obtained by staining with an antibody that recognizes both dephosphorylated cofilin and p-cofilin (Fig. 3A). In starved, resting MTLn3 cells, dephosphorylated cofilin is found in the cytoplasm and in spontaneous protrusions. Upon EGF stimulation, fluorescence intensity analysis (Fig. 3C) confirmed an approximately twofold increase in dephosphorylated cofilin in the leading

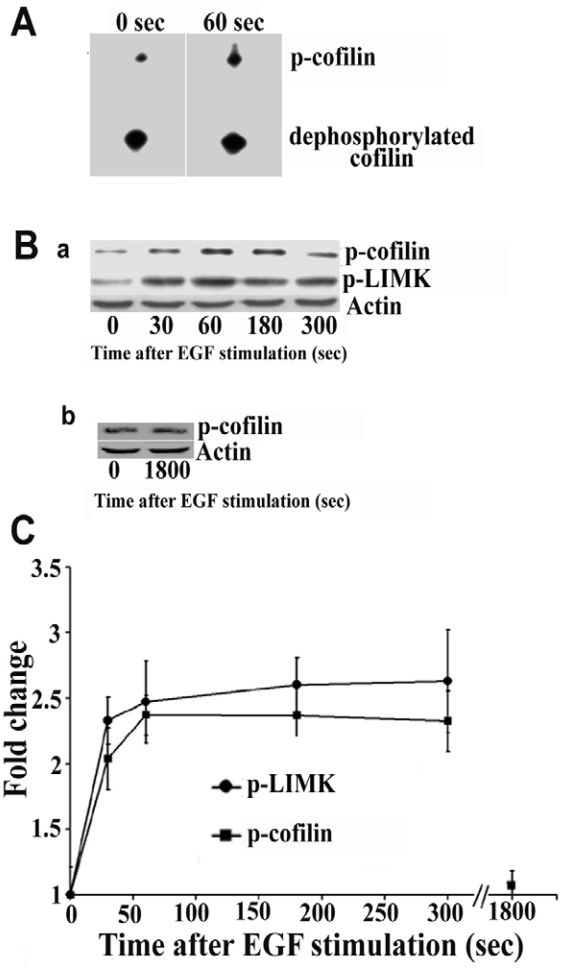

Fig. 2. The majority of cofilin is dephosphorylated in resting cells. (A) Changes in the percentage of p-cofilin in MTLn3 cell lysates at 0 and 60 seconds after stimulation with EGF were analyzed by isoelectric focusing gel electrophoresis (IEF). (B) Time course of p-cofilin and p-LIMK levels in cell lysates after EGF stimulation analyzed by western blotting with anti-p-cofilin and anti-p-LIMK antibodies (a). Change of p-cofilin levels in cell lysates at resting state and 30 minutes after EGF stimulation analyzed by western blotting with anti-p-cofilin antibodies (b). (C) Western blot quantification of the change in p-cofilin and p-LIMK after EGF stimulation standardized to β-actin. (Error bars indicate the s.e.m. based on five independent experiments. The analysis of the representative image shown in Fig. 2B falls within the error bars in Fig. 2C.)

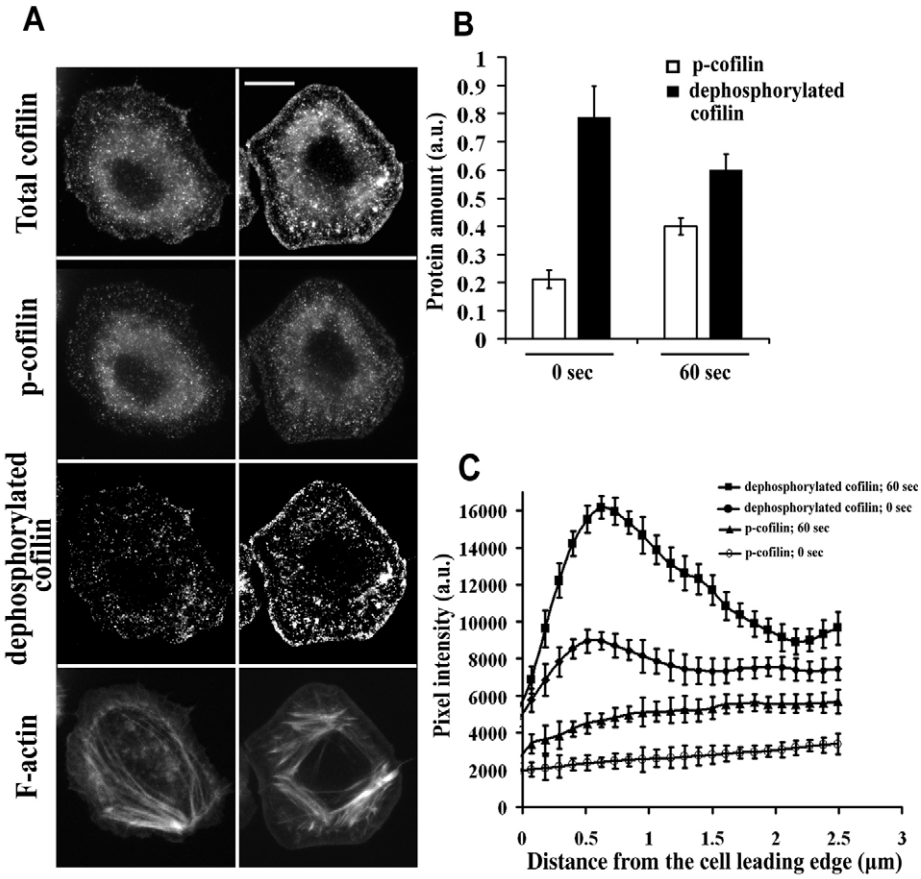

Fig. 3. Dephosphorylation of cofilin does not occur at the leading edge following stimulation with EGF. (A) MTLn3 cells were fixed at 0 and 60 seconds following stimulation with EGF and stained with antibodies against cofilin and p-cofilin. The F-actin cytoskeleton was stained with Alexa Fluor-633-labeled phalloidin. The dephosphorylated cofilin image was prepared by subtracting the scaled p-cofilin image from the total cofilin image using Image J software. (Bar, 10 μm.) (B) Immunofluorescence quantification of dephosphorylated cofilin and p-cofilin throughout the whole cytoplasm of resting and stimulated cells 60 seconds after stimulation with EGF. (Error bars indicate the s.e.m.) (C) Fluorescence intensity analysis of dephosphorylated cofilin and p-cofilin throughout the lamellipod. The lamellipod is defined as the region extending from the cell edge to 2.5 μm into the cell interior, whereas the leading edge is the region where most of the actin nucleation occurs and extends ~1 μm from the membrane (Chan et al., 2000; DesMarais et al., 2002). (Error bars indicate the s.e.m.)

edge of EGF-induced lamellipods, a region extending from the membrane to ~1 μm into the cell interior (Chan et al., 2000; DesMarais et al., 2002).

Furthermore, after EGF stimulation p-cofilin intensity increased approximately twofold by 60 seconds without showing a decrease at the leading edge (Fig. 3B,C). Taken together, these observations argue that dephosphorylation of cofilin does not occur at the leading edge where dephosphorylated cofilin accumulates after stimulation.

Since the peak of cofilin activity at 60 seconds after EGF stimulation (Fig. 1) is required for the early barbed-end transient that occurs at the leading edge at 60 seconds (Mouneimne et al., 2004) and since there is no local dephosphorylation of cofilin at the leading edge, dephosphorylation of cofilin is not spatially coupled to activation of cofilin and might not be the primary mechanism for the initiation of cofilin activation in the lamellipod following the stimulation with growth factor.

Dephosphorylated cofilin but not p-cofilin is associated with the Triton X-100-resistant cytoskeleton

In vitro experiments have shown that p-cofilin does not bind to actin filaments (Ghosh et al., 2004; Meberg and Bamburg, 2000). To investigate the relative binding of dephosphorylated cofilin and p-cofilin to the detergent-resistant cytoskeleton, we analyzed the retention of both forms of cofilin in the Triton X-100-insoluble cytoskeletal fraction in situ by immunofluorescence and in cell lysates by western blotting. Dephosphorylated cofilin was associated with the actin cytoskeleton in both resting and EGF-stimulated cells whereas p-cofilin was not. In addition, dephosphorylated cofilin became associated with filaments in the nucleation zone of the leading edge after EGF stimulation (Fig. 4A). Fractionation of Triton X-100 lysates revealed the presence of cofilin but neither p-cofilin nor LIMK1 in the cytoskeletal pellet fraction (Fig. 4B), confirming our in situ observations. Cofilin was bound to the insoluble cytoskeleton part of the cell after treatment with Triton X-100 ('Triton X-100 residue') and to pellets obtained before or after EGF stimulation, indicating that cofilin is either pre-bound to actin filaments in resting cells and/or associated with detergent-resistant membranes in addition to filaments. Taken together, these data indicate that only the dephosphorylated form of cofilin is associated with the Triton X-100-resistant cytoskeleton and the leading-edge compartment.

LIMK1 and p-cofilin distribution in cells

To investigate the spatial relationship of p-cofilin to its primary kinase, LIMK1, we analyzed the localization of LIMK1 by immunofluorescence relative to p-cofilin in the same cells. LIMK1 was found in a punctate pattern throughout the cytoplasm without any discernable enhancement in any region including the leading edge after EGF stimulation (Fig. 5A,B). Pearson's correlation analysis of LIMK1 and p-cofilin staining patterns did not reveal any significant colocalization in the leading edge before stimulation (Fig. 5C), with a mean correlation value of 0.15. Only a small increase in the correlation value (averaging 0.27 in the leading edge) was observed at 60 seconds following stimulation with EGF, which

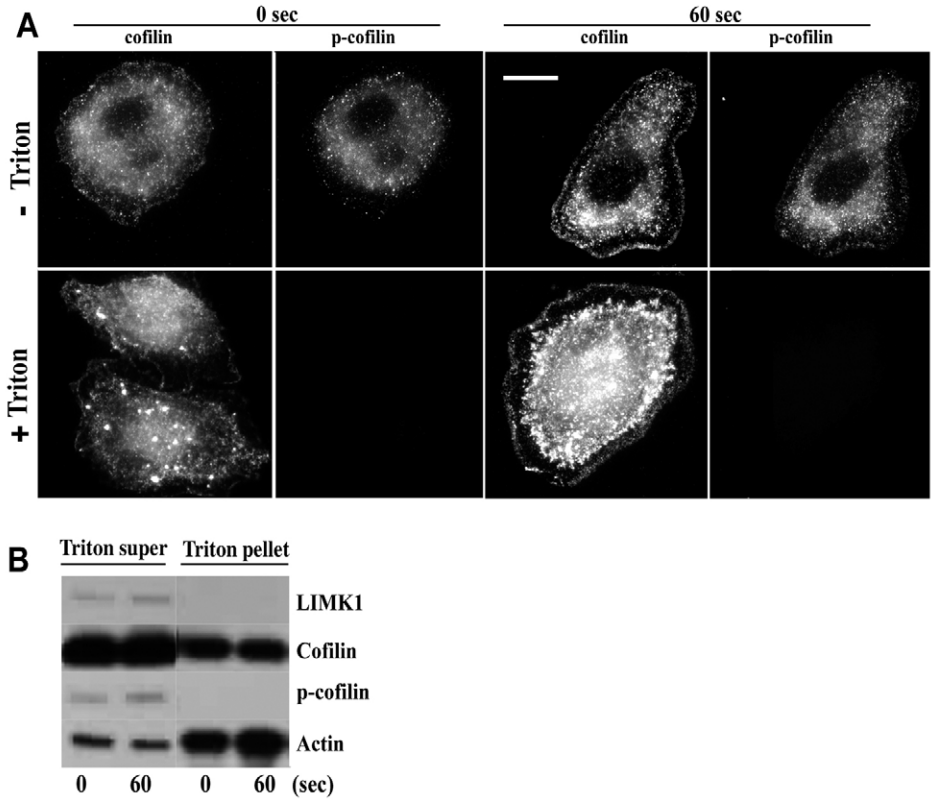

Fig. 4. Dephosphorylated cofilin, but not p-cofilin or LIMK1, is associated with the actin cytoskeleton. (A) Representative immunofluorescence images of cofilin and p-cofilin staining in fixed MTLn3 cells compared with Triton X-100-insoluble cytoskeletons. Cofilin is observed throughout the cytoplasm and in the leading-edge compartment in both non-extracted and Triton X-100-extracted cells. However, p-cofilin is not retained in cells extracted with Triton X-100, indicating that it is not bound to the cytoskeleton. (Bar, 10 μm.) (B) Western blot analysis of the retention of cofilin, p-cofilin and LIMK1 in the Triton X-100-insoluble cytoskeleton of MTLn3 cells at 0 and 60 seconds following stimulation with EGF. Western blot was standardized to total protein.

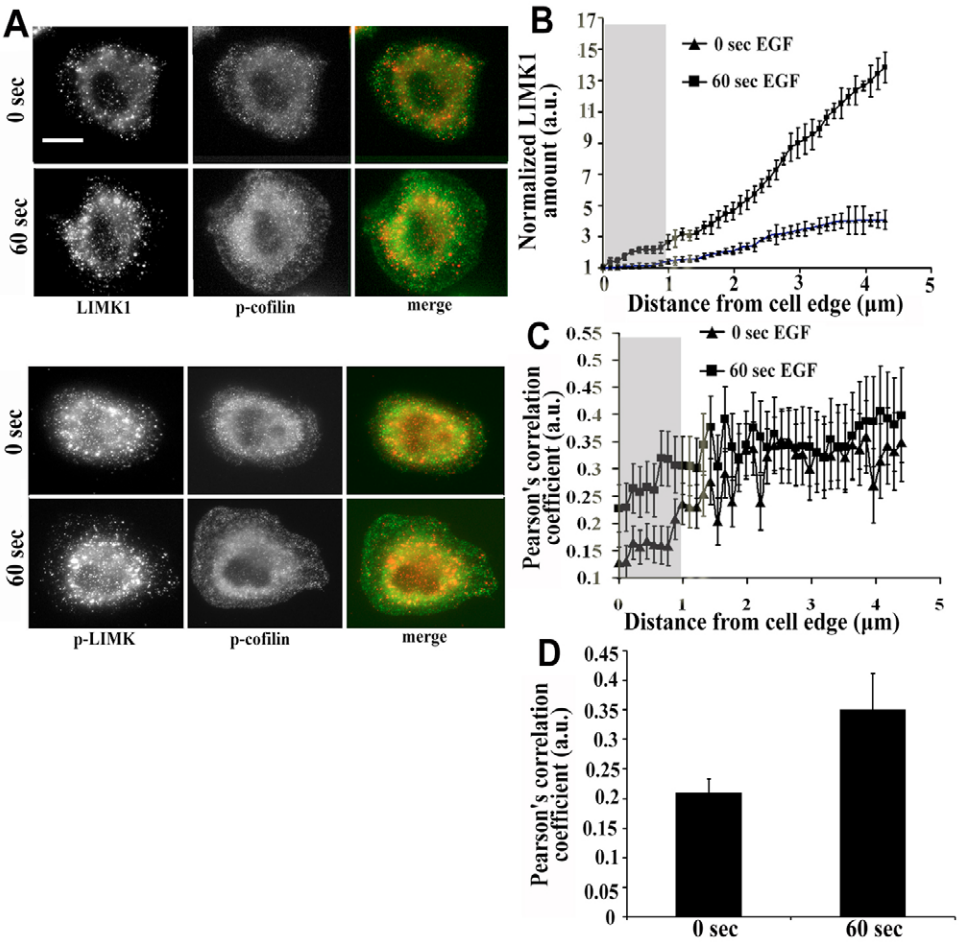

Fig. 5. Distribution of LIMK1 and phosphorylated-cofilin. (A) Representative images of LIMK1, p-LIMK1 and p-cofilin immunolocalization in MTLn3 cells fixed at 0 seconds and 60 seconds following stimulation with EGF. The two localization patterns do not significantly overlap. (Bar, 10 μm.) (B) Analysis of LIMK1 (red) and p-cofilin (green) amount from the membrane to inside of the cell 60 seconds after stimulation with EGF, showing the lack of co-enrichment in the leading edge (shaded). (Error bars indicate the s.e.m.) (C) Pearson's correlation coefficient analysis of the overlap of LIMK1 and p-cofilin channels. Both proteins show a low level of correlation throughout and particularly in the leading edge compartment (shaded) at both before (▲) and 60 seconds after (■) EGF stimulation. (Error bars indicate the s.e.m.) (D) Pearson's correlation coefficient analysis of the overlap of p-LIMK (red) and p-cofilin (green) channels. Both proteins show a low level of correlation in the leading edge compartment both before and after stimulation. (Error bars indicate the s.e.m.)

could be explained as an increase in p-cofilin throughout the cell because it is consistent with the results shown in Fig. 3C. Correlation analysis of LIMK1 phosphorylated on Thr508 (possibly activated) (Ohashi et al., 2000) and p-cofilin yielded similar results to those shown in Fig. 5A-C, with only a small increase (from 0.21 to 0.35) following stimulation with EGF (Fig. 5D). This analysis suggests that LIMK1 phosphorylates cofilin throughout the cell after stimulation and is not colocalized with cofilin before or after stimulation.

EGF-stimulated free barbed ends and lamellipod protrusion do not depend on cofilin phosphorylation status

To investigate the role of cofilin phosphorylation in the actin polymerization and protrusion response elicited by EGF, the ROCK inhibitor Y-27632 – an upstream activator of LIMK – was used. At 60 seconds following stimulation with EGF, a ~40% decrease in the level of LIMK1 phosphorylation was detected in the presence of Y-27632, whereas EGF-stimulated cofilin phosphorylation at 60 seconds was reduced below resting levels (Fig. 6). Therefore, in MTLn3 cells inhibition of ROCK with Y-27632 sufficiently decreases LIMK1 activation to the degree where both the steady-state and EGF-stimulated cofilin phosphorylation levels are suppressed.

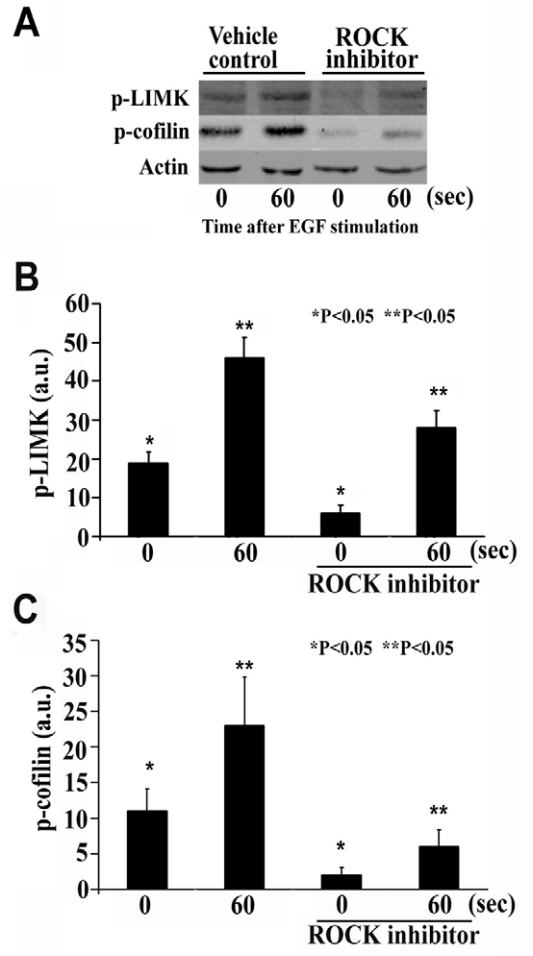

Fig. 6. ROCK-dependent activation of LIMK1 is required for the increase in cofilin phosphorylation following EGF stimulation. (A) MTLn3 cells were preincubated with the ROCK inhibitor Y-27632 (10 μM) for 30 minutes prior to stimulation with EGF. Cell lysates were prepared at 0 and 60 seconds following stimulation with EGF, western blotted and probed with antibodies against p-cofilin and activated p-LIMK. (B,C) Quantification of western blot for changes of LIMK1 and p-cofilin showing the inhibition of LIMK1 and cofilin phosphorylation caused by ROCK inhibitor. (Error bars indicate the s.e.m.)

We next investigated the effect that decreasing levels of p-cofilin by ROCK inhibition have on cell protrusion. No significant differences in either the initial rate or final extent of cell protrusion following EGF stimulation were detected between control and Y-27632-treated cells (Fig. 7). The F-actin pattern in Y-27632-treated cells before and after stimulation with EGF was indistinguishable from control cells (Fig. 7A), whereas analysis of control and Y-27632-treated cells revealed no statistically significant differences in the number of free barbed ends upon EGF stimulation (Fig. 7D). Since the barbed ends generated at 60 seconds following stimulation with EGF are cofilin-dependent (Mouneimne et al., 2004), these data indicate that the approximately twofold increase in cofilin phosphorylation observed in untreated cells is not essential for the generation of cofilin-dependent free barbed ends and lamellipod protrusion at 60 seconds following EGF stimulation.

We also inhibited the EGF-stimulated phosphorylation of cofilin by suppressing LIMK1 expression with small interfering RNA (siRNA). Although LIMK1 expression and cofilin phosphorylation were dramatically suppressed in siRNA treated cells (>85%, Fig. 8A,B), the decrease of p-cofilin level after EGF stimulation did not have any effect on the rate or final extent of cell protrusion (Fig. 8C). Furthermore, LIMK1 siRNA revealed no statistically significant differences in EGF-stimulated barbed end production (Fig. 8D). Both of these results are consistent with those of LIMK inactivation by ROCK inhibition as shown in Fig. 7.

Phospholipase C is not coupled to the cofilin phosphorylation status after stimulation with EGF

Following stimulation of MTLn3 cells with EGF, two distinct transients of free barbed-end creation are observed (Chan et al., 2000). The first transient, occurring at 60 seconds after EGF, requires the activity of cofilin (Fig. 1) and phospholipase C (PLC). Inhibition of PLC by U-73122 inhibits cofilin severing and the 60-seconds barbed-end transient (Mouneimne et al., 2004), confirming that the first barbed-end transient depends on PLC and cofilin.

Previous studies with neutrophils have demonstrated a requirement for PLC activity during the dephosphorylation of cofilin in response to formyl-methionyl-leucyl (fMLF) (Zhan et al., 2003). To determine whether PLC affects cofilin phosphorylation in carcinoma cells, MTLn3 cells were treated with the PLC inhibitor U-73122 or the inactive isoform U-73343 prior to stimulation with EGF. No significant differences between cells treated with PLC inhibitor, the steady-state or EGF-induced levels of p-cofilin were detected (Fig. 9). Thus, although cofilin activation depends on PLC activity (Mouneimne et al., 2004), PLC does not regulate p-cofilin levels during stimulation with EGF, suggesting a separate pathway for PLC regulation of cofilin activity that does not involve changes in cofilin phosphorylation.

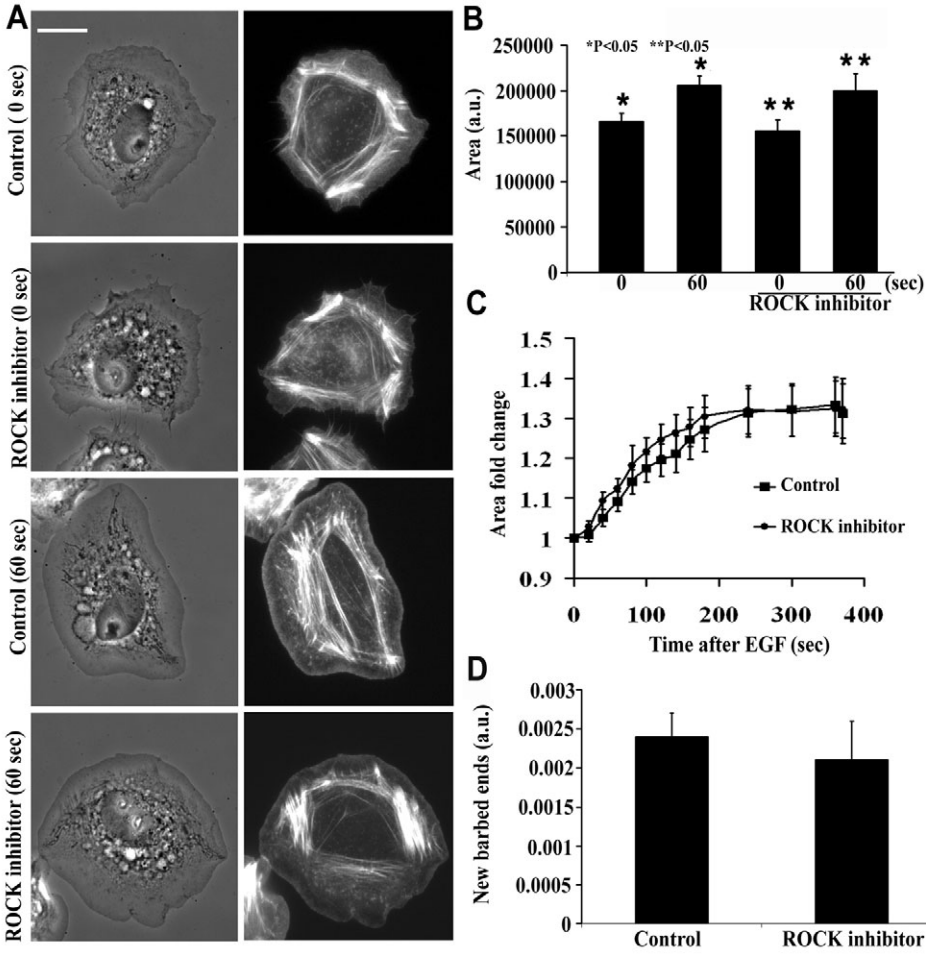

Fig. 7. Phosphorylation of LIMK1 and cofilin is not required for EGF-stimulated lamellipod protrusion and barbed end formation following stimulation with EGF. (A) MTLn3 cells were pre-incubated with the ROCK inhibitor Y-27632 (10 μM) for 30 minutes and fixed at 0 and 60 seconds following stimulation with EGF to inhibit the phosphorylation of both LIMK1 and cofilin. Panel shows representative images of the F-actin cytoskeleton stained with Alexa Fluor-488-labeled phalloidin in control and Y-27632-treated cells. (Bar, 10 μm) (B) The change in lamellipod protrusion area is unaffected by ROCK inhibition. MTLn3 cells were treated with or without the ROCK inhibitor, Y-27632 and fixed at 0 and 60 seconds after stimulation with EGF. The average fold change in cell area measured at 0 and 60 seconds EGF in control and Y-27632-treated cells is identical. Student's *t*-test showed no statistical difference in lamellar protrusion between control and Y-27632 cells. (Error bars indicate the s.e.m.) (C) Time lapse microscopy of MTLn3 cells demonstrate no change in the initial rate or final extent of lamellipod protrusion in Y-27632-treated cells (●) compared with control cells (■) following stimulation with EGF. (D) The change in the appearance of new barbed ends is unaffected by ROCK inhibition. Time lapse microscopy of β-actin-GFP MTLn3 cells demonstrate there is no effect on the fold change in the appearance of new barbed ends in Y-27632-treated cells following stimulation with EGF compared with control cells. For panels C and D, error bars indicate the s.e.m. for nine control cells and 11 Y-27632-treated cells (*n*=2 separate experiments).

Discussion

The wide differences in patterns of cofilin phosphorylation and dephosphorylation during stimulation in different cells types make it difficult to understand the significance of the cofilin phosphorylation cycle in the regulation of cofilin-dependent motility events, such as actin polymerization and protrusion. Because of the importance of cofilin activity in the metastatic behavior of breast carcinoma cells, this study focused on correlating the kinetics of cofilin activation with changes in cofilin phosphorylation in response to EGF for this cell type. Our results show that cofilin-dependent severing is an early event that occurs at the leading edge. Furthermore, the location and timing of cofilin phosphorylation and dephosphorylation is not coupled to cofilin activity at the leading edge. Finally, cofilin phosphorylation is not required for cofilin-dependent barbed-end formation and protrusion. These results support neither a model of dephosphorylation-driven activation of cofilin nor a model in which inactivation of cofilin by phosphorylation is required for cell motility. Instead, our results suggest that the cofilin phosphorylation cycle is not involved directly in the timing and location of cofilin activation. This is consistent with the fact that cofilin appears to have the same functions in *Dictyostelium* amoebae as it does in mammalian cells (Ichetovkin et al., 2000), even though there is no phosphorylation of cofilin in *Dictyostelium* (Bamburg, 1999). These considerations raise questions about the function of cofilin phosphorylation in vivo.

Several observations of our study are useful in determining the regulatory significance of cofilin phosphorylation: (1) Detailed analysis of the fluorescence intensity of p-cofilin staining within the leading edge detected a twofold increase, not a decrease, in p-cofilin upon stimulation with EGF. This is consistent with the increase in p-cofilin observed in cell lysates and effectively rules out dephosphorylation at the leading edge as a mechanism for the initial activation of cofilin severing. (2) Our fluorescence intensity analysis of the leading-edge compartment also revealed that p-cofilin is not depleted within the leading edge in resting cells. It has been reported that non-migratory fibroblasts contain a uniform distribution of p-cofilin at the leading edge, which becomes depleted of p-cofilin during migration (Dawe et al., 2003). By contrast, metastatic carcinoma cells do not show a depletion of p-cofilin at the leading edge. This difference suggests that the location of cofilin phosphorylation is uncoupled from activity. (3) p-cofilin is not associated with the actin cytoskeleton and is, therefore, probably freely diffusible in cells. Likewise, LIMK1 was stained as a uniformly distributed punctate pattern throughout

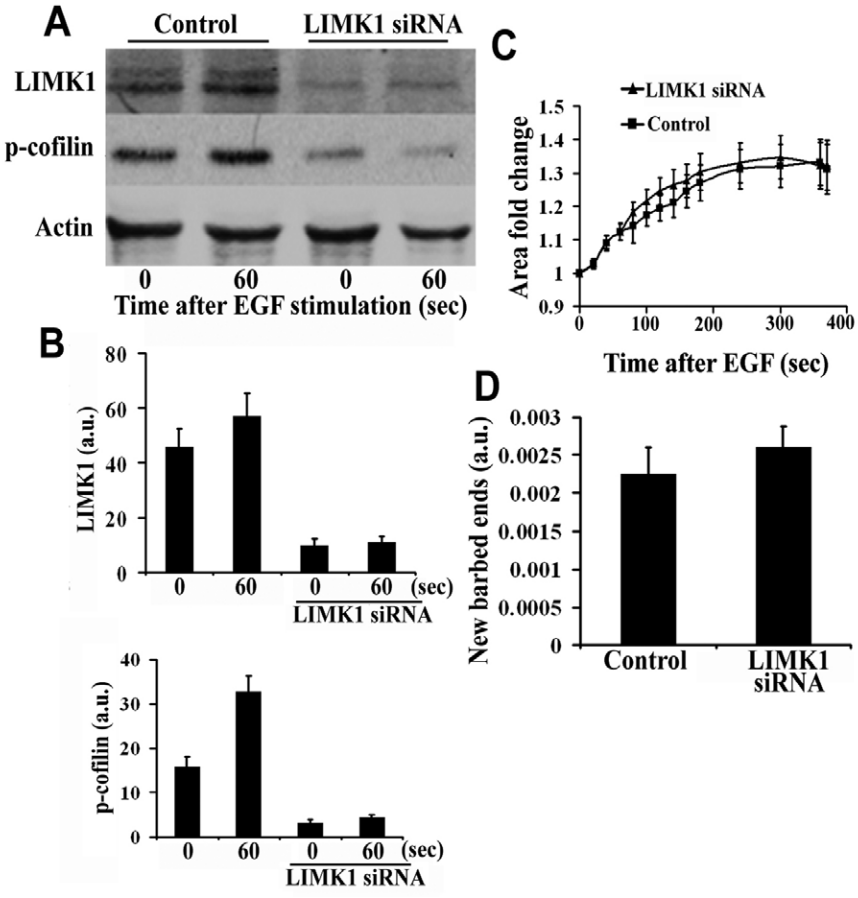

Fig. 8. LIMK1 siRNA has no effect on EGF-stimulated lamellipod protrusion and barbed-end formation. (A) MTLn3 cells were treated with control or LIMK1-specific siRNA oligonucleotides for 36 hours prior to EGF stimulation. Cell lysates were prepared at 0 and 60 seconds following EGF stimulation, western blotted and probed with antibodies against p-cofilin and LIMK-1. (B) Quantification of western blots showing the decrease of LIMK1 expression and cofilin phosphorylation levels in control (left) and LIMK1 siRNA treated cells (right). Error bars indicate the standard error of the mean. (n=3 separate experiments). (C) The change in protrusion area following EGF stimulation of MTLn3 cells is not affected by LIMK1 siRNA treatment. Time lapse microscopy of MTLn3 cells demonstrate no change in the initial rate or final extent of lamellipod protrusion in LIMK1 siRNA-treated cells (▲) compared to control cells (■) following stimulation with EGF. (D) The increase in free barbed ends following EGF stimulation of MTLn3 cells is unaffected in LIMK1 siRNA. Time lapse microscopy of β-actin-GFP MTLn3 cells demonstrate there is no effect on the fold change in the appearance of new barbed ends in LIMK1 siRNA-treated cells following EGF stimulation compared to control cells. For panel C and D, the error bars indicate the s.e.m. (n=2 separate experiments).

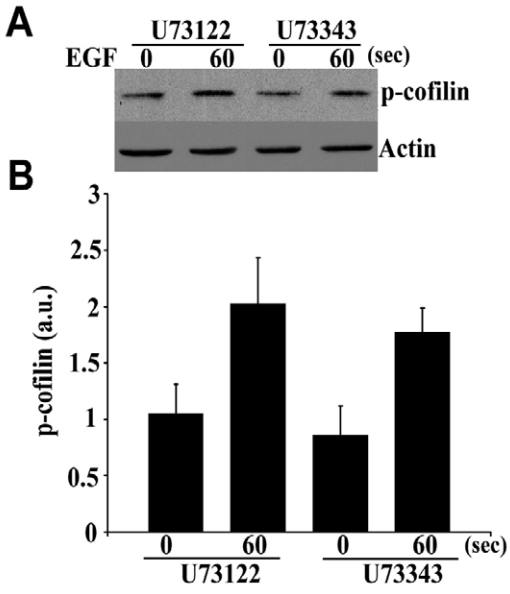

Fig. 9. PLC activation is not required for the increase in p-cofilin levels following EGF. (A) MTLn3 cells were preincubated with the PLC inhibitor U-73312 or the inactive control U-73343 for 10 minutes prior to stimulation with EGF. Cells were lysed at 60 seconds following stimulation with EGF and the amount of p-cofilin measured in western blots. (B) Quantification of the p-cofilin level of western blots. The error bars indicate the s.e.m. (n=2 separate experiments).

the cytoplasm in both resting and stimulated cells. Interestingly, although recombinant LIMK1 has been shown to co-sediment with F-actin in vitro through its C-terminal kinase domain (Yang et al., 1998), we did not detect any association of LIMK1 with the Triton X-100-resistant cytoskeleton, or colocalization of LIMK1 with F-actin contained in stress fibers or filaments of the leading edge. (4) The suppression of p-cofilin levels in cells by the ROCK inhibitor and suppression of LIMK1 by siRNA did not inhibit barbed-end creation or protrusion indicating that cofilin phosphorylation is not required for initiation of motility as proposed elsewhere (Nishita et al., 2002). In addition, we found no evidence for cofilin activation by dephosphorylation during the 60-second transient of cofilin activity following growth factor stimulation of resting carcinoma cells. Previous studies have reported that EGF stimulation of A431 or 3T3 cells did not alter net pADF/pcofilin levels, but increased the phosphorylation and dephosphorylation of cofilin (Meberg et al., 1998). However, the lack of effect of LIM kinase inhibition on cofilin-generated barbed ends indicates that an increase in the turnover of p-cofilin is not involved in the net activation of cofilin. Our result is further supported by the lack of effect on EGF-elicited protrusion and only a minor elevation in cofilin-dependent barbed ends in MTLn3 cells that overexpress a dominant negative LIMK1 containing an inactive kinase domain (KS) compared with control cells (Wang et al., 2006). (5) The induction of a biphasic actin polymerization transient in response to chemoattractant stimulation is a conserved response in chemotactic cells (Chan et al., 1998; Chen et al.,

2003; Cox et al., 1992; Eddy et al., 1997; Funamoto et al., 2002; Hall et al., 1989; Iijima et al., 2002). We have demonstrated that the severing activity of cofilin is required for the early transient of barbed ends and is coupled to PLC activity following EGF stimulation of MTLn3 cells (Mouneimne et al., 2004). However, inhibition of PLC activity did not alter the phosphorylation of cofilin after EGF stimulation indicating that PLC activity and p-cofilin status are uncoupled. This finding suggests an involvement of phosphoinositide hydrolysis during the rapid activation of cofilin-severing following growth factor stimulation that is independent of phosphorylation. In vitro studies have shown that phosphoinositides, specifically PtdIns(4,5)P_2, can bind cofilin and this interaction can prevent F-actin binding (Yonezawa et al., 1990). This finding suggests that a pool of cofilin is held in an inactive state by binding to PtdIns(4,5)P_2 at the membrane in resting cells. Upon stimulation, PtdIns(4,5)P_2 would undergo an increased rate of hydrolysis owing to increase PLC activity, releasing activated cofilin. Gelsolin, a major actin filament capping and severing protein is also regulated by PLC activity. After severing, gelsolin caps the barbed ends until membrane PtdIns(4,5)P_2 levels are restored to cause gelsolin uncapping (Sun et al., 1999). However, the dissociation of gelsolin from barbed ends is a relatively slow process with a half-life of 15 minutes following growth factor stimulation (Allen, 2003). These data are inconsistent with those of gelsolin contributing to the early actin-polymerization transient, which peaks at 1 minute following stimulation with EGF (Chan et al., 2000).

Based on these considerations, what is the significance of the increase in cofilin phosphorylation that occurs in response to stimulation with EGF seen here and in other cell types (Nishita et al., 2005)? It is known that activated cofilin severs actin filaments to generate a heterodimer of cofilin and G-actin that is inhibited from further severing and F-actin-binding events. To recycle cofilin from the heterodimer, either the phosphorylation of cofilin by LIMK or the direct action of cyclase-associated protein (CAP) releases cofilin from G-actin (Balcer et al., 2003; DesMarais, 2004). Since stimulation with EGF causes the activation of LIMK, this method of recycling cofilin might be stimulated in cells in response to EGF. Our results indicate that the phosphorylation of cofilin is spatially and temporally uncoupled from the activity of cofilin. How this recycled cofilin is repositioned for the next round of activation is under investigation. The recent discovery of a complex of all of the key enzymes of the cofilin phosphorylation cycle containing SSH-1L, LIMK1 and 14-3-3ζ (Soosairajah et al., 2005) suggests that the cofilin phosphorylation cycle involves the shuttling of cofilin through a specialized compartment, whose location might determine the repositioning of cofilin.

Materials and Methods

Cell culture

The metastatic rat mammary adenocarcinoma cell line, MTLn3, was cultured in α-MEM medium (Gibco Laboratories) supplemented with 5% fetal bovine serum (FBS) as previously described (Bailly et al., 1998). For light-microscopy experiments, cells were plated on glass bottom MatTek dishes (MatTek Corporation, Ashland, MA), which had been treated with 1 M HCl for 10 minutes, followed by one wash with 95% ethanol, then one wash with PBS. Prior to each experiment, cells were starved in L15 medium (Gibco Laboratories) supplemented with 0.35% BSA (starvation medium), for 3-4 hours. To stimulate cells, MTLn3 cells were treated with a bath application of 5 nM epidermal growth factor (EGF; Invitrogen) for various times.

Reagents and primary antibodies

Y-27632, [(R)-(+)-*trans*-N-(4-pyridyl)-4-(1-aminoethyl)-cyclohexanecarboxamide], 2HCl, a highly selective inhibitor of ROCK was purchased from Calbiochem. U-73122 and U-73343 were obtained from BIOMOL Research Laboratories, Inc. AE765 is a function-blocking rabbit polyclonal antibody generated against a peptide covering both the actin-binding site and the PtdIns(4,5)P_2-binding site of cofilin (Chan et al., 2000). AE774 is a chicken IgY antibody raised against purified recombinant full-length rat cofilin that recognizes both the dephosphorylated and phosphorylated forms of cofilin. AE721 is a guinea pig polyclonal antibody raised against a cofilin-derived peptide containing a phosphorylated Ser residue at position 3 and recognizes exclusively phosphorylated cofilin (p-cofilin), as shown by isoelectric focusing gel analysis. AC-15 is a mouse monoclonal IgG1 antibody that recognizes the β-isoform of actin (Sigma). H-84 is a rabbit polyclonal antibody that recognizes an epitope corresponding to amino acids 136-219 of human LIMK1 (Santa Cruz Biotechnology). A rabbit polyclonal antibody (phospho-LIMK) recognizes LIMK1 and LIMK2 only when phosphorylated at Thr508 or Thr505 (Cell Signaling Technology). IgG fractions of AE765, AE721, AE774 and non-immune rabbit IgG (Sigma) were isolated using T-gel Absorbent (Pierce). All cofilin antibodies were further purified by affinity chromatography against the peptide or protein immunogen.

Immunofluorescence

MTLn3 cells plated on glass-bottom dishes (MatTek Corporation, Ashland, MA) at 30-50% confluence were simultaneously fixed and permeablized as previously described (Eddy et al., 2000). Briefly, cells were fixed in 3.7% paraformaldehyde, 0.1% glutaraldehyde (Electron Microscopy Sciences, Hatfield, PA) and 0.15 mg/ml saponin in Dulbecco's phosphate-buffered saline (PBS). Following a brief rinse in PBS, aldehyde autofluorescence was quenched for 15 minutes with 1 mg/ml $NaBH_4$. Cells were blocked for 1 hour with 1% bovine serum albumin (BSA), 1% FBS in PBS (blocking buffer). For F-actin staining, cells were stained with 0.5 μM Alexa Fluor-488 or -633-conjugated phalloidin (Molecular Probes). Primary antibodies diluted in blocking buffer were incubated with the cells for 1 hour. After rinsing 3× 5 minutes in 1% BSA in PBS, Alexa Fluor-488- or Alexa Fluor-555-conjugated secondary antibodies (Molecular Probes, Eugene, OR) were diluted in blocking buffer and incubated with the cells for 1 hour. Cells were rinsed for 3× 5 minutes in 1% BSA in PBS, 1× 5 minutes in PBS and mounted in 50% glycerol in PBS supplemented with 6 mg/ml n-propyl gallate as an anti-fade agent.

Cofilin activity assay

The relative cofilin severing activity was quantified using modified version of the established light-microscopy severing assay (Chan et al., 2000; Ichetovkin et al., 2000). In brief, MTLn3 cell lysates were prepared by lysing cells (3×10^7 cells/ml) in lysis buffer at different times after stimulation with EGF. Rhodamine and biotin-labeled F-actin were prepared by incubating 0.4 μM Rhodamine-labeled actin, 0.2 μM biotin-labeled actin, and 1.4 μM unlabeled actin in polymerization buffer and 0.2 μM phalloidin for no more than 1.5 hours. Rhodamine and/or biotin-labeled F-actin was diluted 30-fold to 0.67 μM with an anti-bleaching buffer containing 5 mg/ml BSA and anti-bleaching components: 36 ng/ml catalase, 0.2 mg/ml glucose oxidase, and 6 mg/ml glucose and 100 mM DTT in ISAP buffer (20 mM Tris-HCl, pH 7.5, 5 mM EGTA, 2 mM $MgCl_2$, 50 mM KCl, 1 mM ATP, 1 mM DTT). The resulting Rhodamine and biotin-labeled F-actin was then coupled to the beads with an anti-biotin antibody. Anti-biotin antibodies diluted in ISAP buffer were incubated with beads for 10 minutes to make sure that the F-actin filaments attached to the beads are stable and cannot be depolymerized except in response to severing. The severing of actin filaments by cell lysates prepared from MTLn3 cells was observed microscopically [cell lysis buffer: 20 mM Tris-HCl, pH 7.5, 5 mM EGTA, 0.5 mM $MgCl_2$, 0.5% Triton X-100, 0.5 mM ATP, 5 mg/ml BSA, 36 ng/ml catalase, 0.02 mg/ml glucose oxidase, 6 mg/ml glucose, 10 mM DTT, protease inhibitor cocktail set III (Gibco)]. To test the effect of phosphatase inhibitors on the cofilin severing assay, 50 mM NaF and 1 mM Na_3VO_4 were added to the cell lysis buffer. Images of labeled F-actin-coupled beads before and 10 minutes after addition of cell lysate were taken by using the linear range of a CCD camera. Owing to the crosslinking of filaments to the solid surface, the filaments are stable indefinitely and the 20-minute point was used routinely as control check-time to see whether any filament severing occurred in the absence of cofilin. Total bead fluorescence was quantified in ImageJ, and relative cofilin activity was measured as the decrease in fluorescence after adding the lysates as follows:

$$\text{relative cofilin activity} = \frac{\begin{array}{c}(\text{fluorescence intensity after adding lysis buffer alone}) - \\ (\text{fluorescence intensity after adding cell lysate})\end{array}}{(\text{fluorescence intensity after adding lysis buffer alone})}.$$

All cofilin activity measurements were standardized over the total protein content. To determine cofilin dependence of severing a function blocking antibody was used (AE765). For function blocking antibody experiments, cell lysates were incubated with a molar excess of AE765 anti-cofilin IgG or control IgG that does not recognize any protein (non-immune IgG) for 1 hour on ice before addition to labeled F-actin-coupled beads [protein G beads, incubated with anti-biotin antibodies followed by

coating with polymerized F-actin (composed of 0.4 μM Rhodamine-labeled actin, 0.2 μM biotin-labeled actin and 1.4 μM unlabeled actin)].

Colocalizaton analysis

Cells were precisely traced on phase-contrast images. Pixels along the perimeter were measured for intensity correlation. The perimeter was inset by one pixel and measured. This was repeated iteratively to provide Pearson's coefficient from the outer edge of the cell towards the center at 0.22 μm steps. A macro was written in ImageJ 1.32J (Rasband, W.S., Image J, National Institutes of Health, Bethesda, Maryland, USA, http://rsb.info.nih.gov/ij/, 1997-2004) to automate these analyses on the original 16-bit images. The degree of localization was measured as Pearson's correlation coefficient (r) where each element X was a pixel value of one probe and Y the corresponding pixel value of the other probe at the same spatial location and N was the number of perimeter pixels in each annulus:

$$r = \frac{\sum XY - \frac{\sum X \sum Y}{N}}{\sqrt{\left(\sum X^2 - \frac{(\sum X)^2}{N}\right)\left(\sum Y^2 - \frac{(\sum Y)^2}{N}\right)}}.$$

Isoelectric-point analysis

Initial studies from our laboratory reported an average of 48% p-cofilin content in high-density (80% confluent) cultures of resting MTLn3 cells (Zebda et al., 2000). However, evidence gathered in Swiss 3T3 cells (Bernstein et al., 2000) as well as our own recent observations indicated that the p-cofilin content of resting cells is highly sensitive to cell density. MTLn3 cell lysates prepared from cells grown at high-density conditions (80-90% confluent) showed an approximately twofold increase in p-cofilin levels compared with cells grown under low density conditions (30-50% confluent). In light of these observations, a re-examination of the p-cofilin content of resting cells plated at the low density was undertaken. Cells were plated at 30-50% confluence, the confluence used for all stimulation and motility experiments, starved in L15 supplemented with 0.35% BSA (starvation medium) for 3-4 hours. After stimulation with EGF for various time points, the cells were promptly rinsed with cold PBS, and then lysed with sample buffer supplemented with the phosphatase inhibitors 50 mM NaF, 1 mM Na_3VO_4 and protease inhibitor cocktail set III. The lysates were resolved on a Ready Gel pH 3-10 gel (Bio-Rad) and transferred using a semi-dry transfer apparatus (Bio-Rad) to a nitrocellulose membrane. Membranes were blotted with anti-cofilin antibody, followed by anti-rabbit horseradish peroxidase-conjugated secondary antibody, and then visualized using enhanced chemiluminescence (Amersham; Arlington Heights, IL). Densitometric analysis was performed to quantify the bands. In order to ensure that the recovery of cofilin within the lysates is complete, the entire IEF gel was checked for cofilin by western blotting. Cofilin was only detected at its expected isoelectric point (pI=7.8-8.2).

Kinetics of F-actin and barbed-end accumulation at the leading edge

Live MTLn3 cells stably transfected with GFP-β-actin were used and the number of free-barbed ends was quantified as described previously (Lorenz et al., 2004). Briefly, cells were time-lapse imaged on an Olympus IX70 microscope with 60× NA=1.4 infinity-corrected optics coupled to a computer-driven cooled CCD camera using IP lab spectrum software (VayTek). Digital images were linearly converted and the mean fluorescence intensity of each cell was analyzed using a customized macro in NIH image. The number of new filament barbed ends formed at the leading edge is directly proportional to the initial rate of GFP-β-actin incorporation there following stimulation. The slope of the initial edge-intensity increase (the first derivative of GFP-β-actin fluorescence increase) has been documented to be a measure of newly formed barbed ends (Lorenz et al., 2004).

LIMK1 siRNA

Our previous data has established that LIMK1 is the most abundant and dominant cofilin kinase in MTLn3 cells and is upregulated approximately threefold in the invasive subpopulation of carcinoma cells in MTLn3 tumors (Wang et al., 2004). Therefore, suppression of LIMK1 expression with siRNA was performed to reduce the levels of p-cofilin in MTLn3 cells. The siGENOME on-target LIMK1 siRNA duplexes were purchased from Dharmacon RNA Technologies (Chicago, IL) against the following LIMK1 gene sequence: 5′ UUAAGAAGCCGGACCGCAA 3′ (Sense). siRNAs have UU as 3′ overhangs on each strand and a 5′ phosphate on the antisense strand. MTLn3 cells were transfected with the LIMK1 siRNA duplex at 100 nM in the presence of oligofectamine (Invitrogen). The transfection was terminated after 4 hours by addition of 2× serum-containing media. All experiments were performed 36 hours after transfection. The knockdown of LIMK1 was confirmed in cell lysates by western blotting with H-84 rabbit polyclonal antibody and C-10 monoclonal antibody raised against LIMK-1 (Santa Cruz Biotechnology). Control siRNA knockdown experiments included duplexes with either scrambled or irrelevant bacterial sequences as described previously (Mouneimne et al., 2004).

We thank the Analytical Imaging Facility of Albert Einstein College of Medicine for help with all aspects of imaging and data management, especially Michael Cammer for his valuable assistance in image analysis. This work was supported by National Institute of Health grants GM38511.

References

Allen, P. G. (2003). Actin filament uncapping localizes to ruffling lamellae and rocketing vesicles. *Nat. Cell Biol.* **5**, 972-979.

Bailly, M., Condeelis, J. S. and Segall, J. E. (1998). Chemoattractant-induced lamellipod extension. *Microsc. Res. Tech.* **43**, 433-443.

Balcer, H. I., Goodman, A. L., Rodal, A. A., Smith, E., Kugler, J., Heuser, J. E. and Goode, B. L. (2003). Coordinated regulation of actin filament turnover by a high-molecular-weight Srv2/CAP complex, cofilin, profilin, and Aip1. *Curr. Biol.* **13**, 2159-2169.

Bamburg, J. R. (1999). Proteins of the ADF/cofilin family: essential regulators of actin dynamics. *Annu. Rev. Cell Dev. Biol.* **15**, 185-230.

Bernstein, B. W., Painter, W. B., Chen, H., Minamide, L. S., Abe, H. and Bamburg, J. R. (2000). Intracellular pH modulation of ADF/cofilin proteins. *Cell Motil. Cytoskeleton* **47**, 319-336.

Chan, A. Y., Raft, S., Bailly, M., Wyckoff, J. B., Segall, J. E. and Condeelis, J. S. (1998). EGF stimulates an increase in actin nucleation and filament number at the leading edge of the lamellipod in mammary adenocarcinoma cells. *J. Cell Sci.* **111**, 199-211.

Chan, A. Y., Bailly, M., Zebda, N., Segall, J. E. and Condeelis, J. S. (2000). Role of cofilin in epidermal growth factor-stimulated actin polymerization and lamellipod protrusion. *J. Cell Biol.* **148**, 531-542.

Chen, L., Janetopoulos, C., Huang, Y. E., Iijima, M., Borleis, J. and Devreotes, P. N. (2003). Two phases of actin polymerization display different dependencies on PI(3,4,5)P3 accumulation and have unique roles during chemotaxis. *Mol. Biol. Cell* **14**, 5028-5037.

Condeelis, J. (2001). How is actin polymerization nucleated in vivo? *Trends Cell Biol.* **11**, 288-293.

Cox, D., Condeelis, J., Wessels, D., Soll, D., Kern, H. and Knecht, D. A. (1992). Targeted disruption of the ABP-120 gene leads to cells with altered motility. *J. Cell Biol.* **116**, 943-955.

Dawe, H. R., Minamide, L. S., Bamburg, J. R. and Cramer, L. P. (2003). ADF/cofilin controls cell polarity during fibroblast migration. *Curr. Biol.* **13**, 252-257.

DesMarais, V., Ichetovkin, I., Condeelis, J. and Hitchcock-DeGregori, S. E. (2002). Spatial regulation of actin dynamics: a tropomyosin-free, actin-rich compartment at the leading edge. *J. Cell Sci.* **115**, 4649-4660.

DesMarais, V., Ghosh, M., Eddy, R. E. and Condeelis, J. (2004). Cofilin takes the lead. *J. Cell Sci.* **118**, 19-26.

Du, J. and Frieden, C. (1998). Kinetic studies on the effect of yeast cofilin on yeast actin polymerization. *Biochemistry* **37**, 13276-13284.

Eddy, R. J., Han, J. and Condeelis, J. S. (1997). Capping protein terminates but does not initiate chemoattractant-induced actin assembly in Dictyostelium. *J. Cell Biol.* **139**, 1243-1253.

Eddy, R. J., Pierini, L. M., Matsumura, F. and Maxfield, F. R. (2000). Ca2+-dependent myosin II activation is required for uropod retraction during neutrophil migration. *J. Cell Sci.* **113**, 1287-1298.

Edwards, D. C., Sanders, L. C., Bokoch, G. M. and Gill, G. N. (1999). Activation of LIM-kinase by Pak1 couples Rac/Cdc42 GTPase signalling to actin cytoskeletal dynamics. *Nat. Cell Biol.* **1**, 253-259.

Funamoto, S., Meili, R., Lee, S., Parry, L. and Firtel, R. A. (2002). Spatial and temporal regulation of 3-phosphoinositides by PI 3-kinase and PTEN mediates chemotaxis. *Cell* **109**, 611-623.

Ghosh, M., Ichetovkin, I., Song, X., Condeelis, J. S. and Lawrence, D. S. (2002). A new strategy for caging proteins regulated by kinases. *J. Am. Chem. Soc.* **124**, 2440-2441.

Ghosh, M., Song, X., Mouneimne, G., Sidani, M., Lawrence, D. S. and Condeelis, J. S. (2004). Cofilin promotes actin polymerization and defines the direction of cell motility. *Science* **304**, 743-746.

Gohla, A., Birkenfeld, J. and Bokoch, G. M. (2005). Chronophin, a novel HAD-type serine protein phosphatase, regulates cofilin-dependent actin dynamics. *Nat. Cell Biol.* **7**, 21-29.

Hall, A. L., Warren, V. and Condeelis, J. (1989). Transduction of the chemotactic signal to the actin cytoskeleton of Dictyostelium discoideum. *Dev. Biol.* **136**, 517-525.

Ichetovkin, I., Han, J., Pang, K. M., Knecht, D. A. and Condeelis, J. S. (2000). Actin filaments are severed by both native and recombinant dictyostelium cofilin but to different extents. *Cell Motil. Cytoskeleton* **45**, 293-306.

Iijima, M., Huang, Y. E. and Devreotes, P. (2002). Temporal and spatial regulation of chemotaxis. *Dev. Cell* **3**, 469-478.

Kanamori, T., Hayakawa, T., Suzuki, M. and Titani, K. (1995). Identification of two 17-kDa rat parotid gland phosphoproteins, subjects for dephosphorylation upon beta-adrenergic stimulation, as destrin- and cofilin-like proteins. *J. Biol. Chem.* **270**, 8061-8067.

Lorenz, M., DesMarais, V., Macaluso, F., Singer, R. H. and Condeelis, J. (2004).

Measurement of barbed ends, actin polymerization, and motility in live carcinoma cells after growth factor stimulation. *Cell Motil. Cytoskeleton* **57**, 207-217.

Maciver, S. K., Pope, B. J., Whytock, S. and Weeds, A. G. (1998). The effect of two actin depolymerizing factors (ADF/cofilins) on actin filament turnover: pH sensitivity of F-actin binding by human ADF, but not of Acanthamoeba actophorin. *Eur. J. Biochem.* **256**, 388-397.

Maekawa, M., Ishizaki, T., Boku, S., Watanabe, N., Fujita, A., Iwamatsu, A., Obinata, T., Ohashi, K., Mizuno, K. and Narumiya, S. (1999). Signaling from Rho to the actin cytoskeleton through protein kinases ROCK and LIM-kinase. *Science* **285**, 895-898.

Meberg, P. J. and Bamburg, J. R. (2000). Increase in neurite outgrowth mediated by overexpression of actin depolymerizing factor. *J. Neurosci.* **20**, 2459-2469.

Meberg, P. J., Ono, S., Minamide, L. S., Takahashi, M. and Bamburg, J. R. (1998). Actin depolymerizing factor and cofilin phosphorylation dynamics: response to signals that regulate neurite extension. *Cell Motil. Cytoskeleton* **39**, 172-190.

Moriyama, K., Iida, K. and Yahara, I. (1996). Phosphorylation of Ser-3 of cofilin regulates its essential function on actin. *Genes Cells* **1**, 73-86.

Mouneimne, G., Soon, L., DesMarais, V., Sidani, M., Song, X., Yip, S. C., Ghosh, M., Eddy, R., Backer, J. M. and Condeelis, J. (2004). Phospholipase C and cofilin are required for carcinoma cell directionality in response to EGF stimulation. *J. Cell Biol.* **166**, 697-708.

Nishita, M., Aizawa, H. and Mizuno, K. (2002). Stromal cell-derived factor 1alpha activates LIM kinase 1 and induces cofilin phosphorylation for T-cell chemotaxis. *Mol. Cell Biol.* **22**, 774-783.

Nishita, M., Tomizawa, C., Yamamoto, M., Horita, Y., Ohashi, K. and Mizuno, K. (2005). Spatial and temporal regulation of cofilin activity by LIM kinase and Slingshot is critical for directional cell migration. *J. Cell Biol.* **171**, 349-359.

Niwa, R., Nagata-Ohashi, K., Takeichi, M., Mizuno, K. and Uemura, T. (2002). Control of actin reorganization by Slingshot, a family of phosphatases that dephosphorylate ADF/cofilin. *Cell* **108**, 233-246.

Ohashi, K., Nagata, K., Maekawa, M., Ishizaki, T., Narumiya, S. and Mizuno, K. (2000). Rho-associated kinase ROCK activates LIM-kinase 1 by phosphorylation at threonine 508 within the activation loop. *J. Biol. Chem.* **275**, 3577-3582.

Ojala, P. J., Paavilainen, V. and Lappalainen, P. (2001). Identification of yeast cofilin residues specific for actin monomer and PIP2 binding. *Biochemistry* **40**, 15562-15569.

Okada, K., Takano-Ohmuro, H., Obinata, T. and Abe, H. (1996). Dephosphorylation of cofilin in polymorphonuclear leukocytes derived from peripheral blood. *Exp. Cell Res.* **227**, 116-122.

Ono, S., Abe, H., Nagaoka, R. and Obinata, T. (1993). Colocalization of ADF and cofilin in intranuclear actin rods of cultured muscle cells. *J. Muscle Res. Cell Motil.* **14**, 195-204.

Pollard, T. D. and Borisy, G. G. (2003). Cellular motility driven by assembly and disassembly of actin filaments. *Cell* **112**, 453-465.

Soosairajah, J., Maiti, S., Wiggan, O., Sarmiere, P., Moussi, N., Sarcevic, B., Sampath, R., Bamburg, J. R. and Bernard, O. (2005). Interplay between components of a novel LIM kinase-slingshot phosphatase complex regulates cofilin. *EMBO J.* **24**, 473-486.

Sun, H. Q., Yamamoto, M., Mejillano, M. and Yin, H. L. (1999). Gelsolin, a multifunctional actin regulatory protein. *J. Biol. Chem.* **274**, 33179-33182.

Wang, W., Goswami, S., Lapidus, K., Wells, A. L., Wyckoff, J. B., Sahai, E., Singer, R. H., Segall, J. E. and Condeelis, J. S. (2004). Identification and testing of a gene expression signature of invasive carcinoma cells within primary mammary tumors. *Cancer Res.* **64**, 8585-8594.

Wang, W., Mouneimne, G., Sidani, M., Wyckoff, J., Chen, X., Makris, A., Goswami, S., Bresnick, A. R. and Condeelis, J. S. (2006). The activity status of cofilin is directly related to invasion, intravasation, and metastasis of mammary tumors. *J. Cell Biol.* **173**, 395-404.

Yang, N., Higuchi, O., Ohashi, K., Nagata, K., Wada, A., Kangawa, K., Nishida, E. and Mizuno, K. (1998). Cofilin phosphorylation by LIM-kinase 1 and its role in Rac-mediated actin reorganization. *Nature* **393**, 809-812.

Yonezawa, N., Nishida, E., Iida, K., Yahara, I. and Sakai, H. (1990). Inhibition of the interactions of cofilin, destrin, and deoxyribonuclease I with actin by phosphoinositides. *J. Biol. Chem.* **265**, 8382-8386.

Yonezawa, N., Homma, Y., Yahara, I., Sakai, H. and Nishida, E. (1991). A short sequence responsible for both phosphoinositide binding and actin binding activities of cofilin. *J. Biol. Chem.* **266**, 17218-17221.

Zebda, N., Bernard, O., Bailly, M., Welti, S., Lawrence, D. S. and Condeelis, J. S. (2000). Phosphorylation of ADF/cofilin abolishes EGF-induced actin nucleation at the leading edge and subsequent lamellipod extension. *J. Cell Biol.* **151**, 1119-1128.

Zhan, Q., Bamburg, J. R. and Badwey, J. A. (2003). Products of phosphoinositide specific phospholipase C can trigger dephosphorylation of cofilin in chemoattractant stimulated neutrophils. *Cell Motil. Cytoskeleton* **54**, 1-15.

Journal of Cell Science